WATER RESOURCES RESEARCH, VOL. 26, NO. 9, PAGES 1951–1960, SEPTEMBER 1990

Experimental Testing of Transient Unsaturated Flow Theory at Low Water Content in a Centrifugal Field

JOHN R. NIMMO

Water Resources Division, U.S. Geological Survey, Menlo Park, California

Experimental measurements and theoretical predictions of transient moisture conditions have been compared for a sandy soil approaching hydrostatic equilibrium in a centrifugal field. Starting near saturation, samples were centrifuged at constant speed with a constant suction at the outflow boundary. Water flowed freely out of the sample through a porous plate. Step increases in centrifuge speed produced transient moisture conditions suitable for comparison between experiment and theory. Measurements of electrical conductivity by a direct contact four-electrode technique indicated the water content according to a calibration based on known moisture conditions at various equilibrium states. A specially modified centrifuge permitted electrical measurements during centrifugation. For comparison, the transient water contents were computed by a finite-difference solution of Richards' equation (modified by replacing gravitational with centrifugal potential), using soil characteristics measured previously by steady state techniques. The time dependence of water content changes, used as the basis for comparison between experiment and theory, shows agreement which is reasonable given the degree of uncertainty of the measurements. The experiment confirms, within a factor of 4, the validity of Richards' equation for moisture conditions as dry as 25% of saturation, over a hydraulic conductivity range of 5×10^{-11} to 1×10^{-8} m/s, and in a centrifugal field up to about 200 g.

INTRODUCTION

Incorporating Darcy's law and the condition of continuity, Richards' equation encapsulates the generally accepted theory of transient flow in an unsaturated porous medium. Virtually every quantitative approach to unsaturated-zone hydrology relies on the validity of this equation. Expressed mathematically in one dimension for flow driven by pressure gradients and gravity, Richards' equation is

$$\frac{d\theta}{d\psi}\frac{\partial\psi}{\partial t} = \frac{\partial}{\partial z}\left(K\frac{\partial\psi}{\partial z}\right) + \rho g\frac{\partial K}{\partial z} \tag{1}$$

where θ is volumetric water content, ψ is matric potential, t is time, z is the vertical space coordinate, K is hydraulic conductivity considered as a function of ψ or θ, ρ is the density of water, and g is gravitational acceleration. Though (1) represents generally accepted theory, its validity can be rigorously established only by experimental tests that compare its predictions with measured results obtained independently of the parameters used in computation.

Equation (1) is a combination of the continuity equation and Darcy's law applied to the total potential

$$\Phi_g = \psi + \rho g z \tag{2}$$

where the subscript refers to the gravitational case. When the body force driving flow is centrifugal, it is necessary to replace the total potential with

$$\Phi_c = \psi - \tfrac{1}{2}\rho\omega^2 r^2 \tag{3}$$

where ω is the angular speed of rotation and r is the distance from the center of rotation. Then Richards' equation takes the form

$$\frac{d\theta}{d\psi}\frac{\partial\psi}{\partial t} = \frac{\partial}{\partial r}\left(K\frac{\partial\psi}{\partial r}\right) - \rho\omega^2\frac{\partial}{\partial r}(rK) \tag{4}$$

in which the key differences are the change from coordinate z to r and the alteration in the body force term at the extreme right.

Equation (4) is valuable even though it does not apply directly to natural systems. Various transient measurement techniques for unsaturated or multiphase flow characteristics directly involve centrifugal fields [e.g., *Alemi et al.*, 1976; *Hagoort*, 1980; *van Spronsen*, 1982]. Centrifugal techniques for geotechnical modeling commonly apply to situations of transient unsaturated flow, several examples of which are described by *Schofield* [1980]. It is possible to develop inverse methods for determining flow characteristics from easily measured transient flow quantities in a centrifuge, as is now commonly done with pressure- and gravity-driven flow [*Kool et al.*, 1987]. One such technique was proposed by *Alemi et al.* [1976]. In all of these applications, the use of centrifugal force is desirable because it allows faster operation, greater accuracy, or a wider range of water content than would otherwise be possible.

Certain physical attributes of centrifugally driven flow are unique. As is clear from its r dependence, the centrifugal force is spatially nonuniform, though in general this complicates the descriptive mathematics without substantially altering basic physical phenomena. Normally the most critical difference is the great body force possible in a centrifuge. In most applications this force dominates all other forces driving the flow, unlike the noncentrifugal cases where pressure gradients can easily overwhelm gravity. Besides driving flow faster than usual for a given moisture state, the great body force may also affect the shape of air-water interfaces and the microscale distribution of water. *Nimmo et al.* [1987] provided evidence that Darcy's law remains valid under these conditions, but this evidence applies only to steady state flow.

Experimental tests of Richards' equation in the form of (4)

Paper number 90WR00991.

are essential to establish the validity of centrifugal measuring and modeling techniques that quantify transient flow conditions. Moreover, additional tests of this equation in any form are needed to cover the wide variety of conditions in which moisture flow takes place in porous media. The importance of rigor, variety, and number of such tests has increased with the growing use of inverse methods for $K(\theta)$ and $\theta(\psi)$ determination, which rely on the universal validity of Richards' equation. For this purpose the use of a centrifuge can afford the same speed, accuracy, and θ range advantages that it provides in other porous media experiments.

Several published studies have compared numerical solutions of (1) with measured results. Because there are many ways to categorize these studies (medium; conditions tested, e.g., drying, wetting, infiltration, evaporation; compared quantity; moisture range; etc.), each one is unique. Most show good agreement of experiment and theory [e.g., *Staple*, 1969; *Bresler et al.*, 1969; *Luthin et al.*, 1975; *Hoa et al.*, 1977]. A typical example is the study of *Bresler et al.* [1969], involving column experiments in which a clay loam was subjected successively to infiltration, redistribution, and evaporation. The water content at a given depth during redistribution was both measured and computed by a finite difference solution of Richards' equation [*Hanks et al.*, 1969]. The K data used in computation were derived from an evaluation of the transient flow during the evaporation stage of the same experiments. Comparison of $\theta(t)$ for experiment and theory showed "the same general trend in change of water content with time" [*Bresler et al.*, 1969, p. 836].

The strongest tests are generally those in which the necessary K and $\theta(\psi)$ values are measured independently of the measurements which are compared with theory [*Freeze and Banner*, 1970; *Tang and Skaggs*, 1977; *Gilham et al.*, 1979; *Kunze and Nielsen*, 1983]. These mostly show acceptable agreement with Richards' equation, though not quite as close as in other tests. One exception is the study of *Kunze and Nielsen* [1983], which showed only fair agreement at best, explained as probably resulting from the difficulty of obtaining accurate K and $\theta(\psi)$ measurements. *Gilham et al.* [1979] conducted a particularly rigorous experiment and found good agreement with theory. Some studies have used steady state methods for the necessary K measurements. *Freeze and Banner* [1970] and *Tang and Skaggs* [1977] did so and found reasonable, but not outstanding, agreement. Thus these existing reports have no substantial evidence against the validity of Richards' equation. They are limited, however, in several respects, most notably in considering soils only under wet conditions. K values in these tests did not go much lower than 10^{-6} m/s.

The objectives of the present experiment were to rigorously test Richards' equation under low-θ, low-K (10^{-8} to 10^{-10} m/s) conditions by direct measurement of transient moisture states during centrifugation. This was to be done with a medium whose $K(\theta)$ and $\theta(\psi)$ characteristics were well established in previous studies and for which replicate samples were available. The transient moisture response in the centrifuge was to involve a $\theta(t)$ that could be measured and also computed from (4). Then experiment and theory could be compared to see if they agree within limits appropriate for the measurement error and the adequacy of necessary approximations and assumptions.

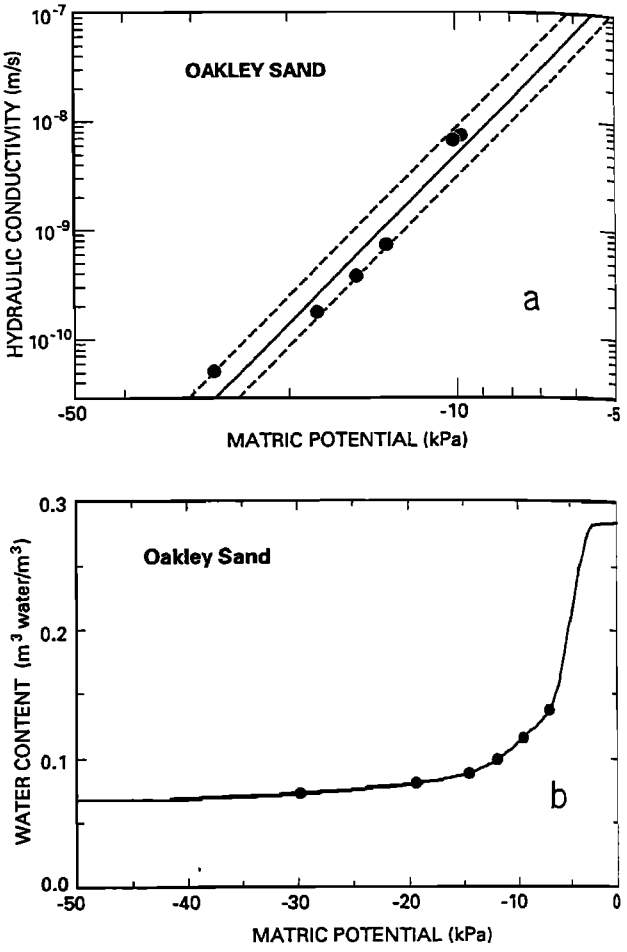

Fig. 1. Unsaturated moisture characteristics of Oakley sand. (*a*) Hydraulic conductivity versus matric potential. The points are measurements by the steady state centrifuge method. The solid curve is a least squares fit to the empirical formula $K(\psi) = K_{sat}/[\psi/\psi_a]^m + 1]$, with $K_{sat} = 1.277 \times 10^{-5}$ m/s, $\psi_a = -2.0940$ kPa and $m = 4.9577$. The dashed curves define a range within which all the measurements fall. (*b*) Water content versus matric potential: measured points interpolated and extrapolated as by *Nimmo and Akstin* [1988].

EXPERIMENT

The general experimental plan was to generate outflow from wet soil in a centrifugal field, increasing the speed in steps so that after each increase there is additional outflow as the soil water responds to the greater force. With known flow characteristics, it is easy to calculate $\theta(t, r)$ using the centrifugal Richards' equation, (4). For the comparison, electrical conductivity (σ) was to be measured in small portions of the sample and used as an indication of $\theta(t)$. The difficulty of making these measurements during centrifugation was solved with a new custom-modified centrifuge.

The soil used in this experiment was Oakley sand, whose $K(\psi)$ and $\theta(\psi)$ characteristics (Figure 1) were measured previously under far-from-saturated conditions by *Nimmo et al.* [1987] and *Nimmo and Akstin* [1988] using the steady state centrifuge method. Because these measurements were made under steady state conditions, their validity requires no presumptions concerning transient flow theory, thus maintaining the independence necessary for a rigorous test. Although only drying curves were available, there are no

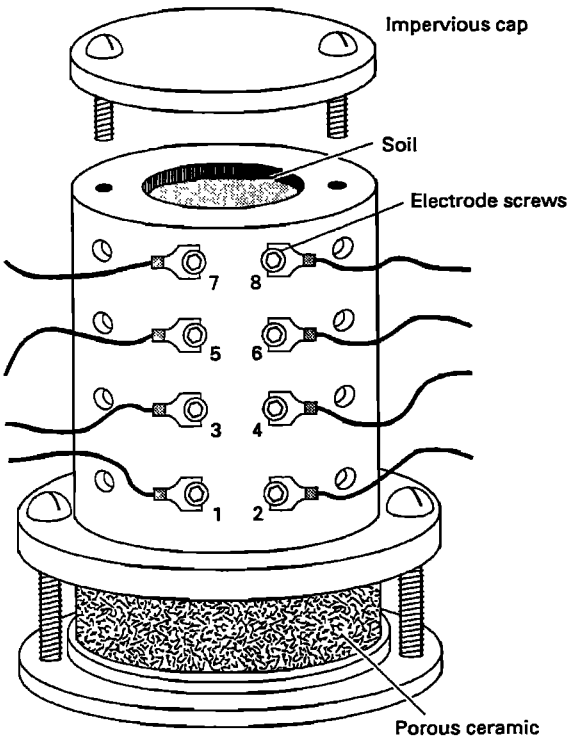

Fig. 2. The soil retainer used for testing Richards' equation during centrifugation. Screws numbered 1 through 8 make three curved square four-electrode configurations for measuring σ at three positions in the sample. The porous ceramic plate and bottom support plate with overflow lip establish, at equilibrium, a constant suction condition at the bottom surface of the soil.

hysteresis problems in the present study because all measured θ changes went from wetter to drier. The soil was densely packed using an automated packing machine [*Ripple et al.*, 1973] and compacted in the centrifuge at 1910 g, thus following the procedure designated "D2F2C2" in the notation of *Nimmo and Akstin* [1988]. In order to have room in the centrifuge bucket for wires and electrodes, the soil sample was recored to a smaller diameter (25.4 mm), retaining its 38 mm height. The water used to wet the sample during preparation and before each experimental run was selenate solution (0.01 N $CaSO_4$ and 0.01 N $CaSeO_4$) with electrical conductivity equal to 1.43 dS/m at the laboratory temperature of 22°C.

Apparatus

The centrifuge was a Beckman Instruments model J6-M specially modified at the factory to incorporate on top of the rotor a Meridian Laboratory MM12 high-speed, low-noise rotating electrical contractor. (Use of brand names is for identification purposes only and does not constitute endorsement by the U.S. Geological Survey.) This equipment permits 12 wires attached to devices in a rotating bucket to be in continuous electrical contact with wires leading to electronic devices outside the centrifuge.

The apparatus placed in the centrifuge buckets included the soil in its retainer, shown in Figure 2, and a reservoir at the bottom to collect outflowing water. A ceramic plate with a water table maintained about 10 mm below the bottom of the sample established a constant (for given ω) negative matric potential at the outflow boundary of the soil. The top of the sample was capped, though not with an airtight seal.

The soil retainer was made of Delrin, chosen for electrical insulation, adequate rigidity, and negligible effect on surface tension (tested using a platinum ring measuring device and following procedures used by *Topp* [1966]). Threaded holes held stainless steel screws, 4 mm in diameter, used as electrodes. The screws were long enough to protrude slightly (0.5–1 mm) into the soil. Of the retainer's 32 holes, those not in use at any time were plugged with stainless steel set screws. A small thin-film platinum resistive temperature detector (RTD) was attached to the outside of the retainer for temperature measurements.

For the electrical conductivity measurements, a curved variation of the square four-electrode arrangement [*Habberjam*, 1979] was developed because the spatial resolution of linear [e.g., *Kirkham and Taylor*, 1950] and circumferential [e.g., *Gupta and Hanks*, 1972] four-electrode arrays proved to be inadequate. The curved square arrangement used here has two rows of two screws 45° apart on the circumference, with a 7.6-mm vertical spacing (center to center) of the screws. As shown in Figure 2, the use of eight screws in two vertical rows allows measurement using three different four-electrode sets. Electrodes 1, 2, 3, and 4 comprise the lower electrode set; 3, 4, 5, and 6 the middle set; and 5, 6, 7, and 8 the upper set.

To make electrical conductivity measurements by the four-electrode method, a measured ac signal (5 V, 37 Hz) supplied current to two electrodes while the potential difference between the other two electrodes was measured. The signal voltage was selected to be great enough to minimize effects of noise without causing undue heating or other unwanted effects on the sample. The frequency was chosen to be low enough that stray capacitances and inductances would not be a serious problem and high enough that sampling rates could be reasonably fast and to be distinctly different from 60-Hz background signals. A digital voltmeter indicated the current by reading the voltage across a precision resistor in series with the current electrodes. The same voltmeter read the voltage across the potential electrodes. A matrix switch in an electronic scanner (Keithley model 706 with model 7052 scanner cards) permitted connections between any wire from the centrifuge and any of the devices (signal generator, voltmeter, etc.) outside. A small computer controlled the scanner and recorded the measurements.

The ratio of the measured potential difference to the supplied current is taken as the configuration resistance. For a four-electrode arrangement, there are three possible independent pairings of electrodes (taking the current electrodes, say, as a vertical, horizontal, or diagonal pair) that give three different values of resistance. For ideal apparatus the sum of two of these equals the third [*Carpenter*, 1955], so the sum of the three different measurements, divided by two, will give an average effective measurement of overall configuration resistance. A value, symbolized R, was obtained this way each time an electrode set was read.

The configuration resistance determines electrical conductivity very simply according to

$$\sigma = U/R \tag{5}$$

where U is the cell constant. The value of U was obtained by measuring R with a conductive liquid (a gelatine solution,

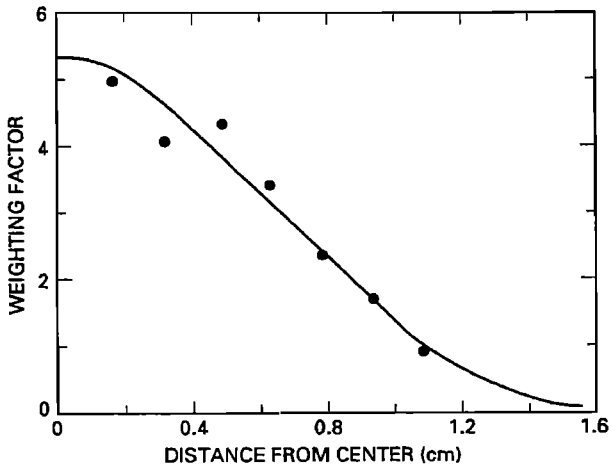

Fig. 3. The weighting factor w, illustrating the sensitivity of a curved square electrode set as a function of the distance x from the center of the electrodes. The solid curve is a least squares fit of (7) to the measured data.

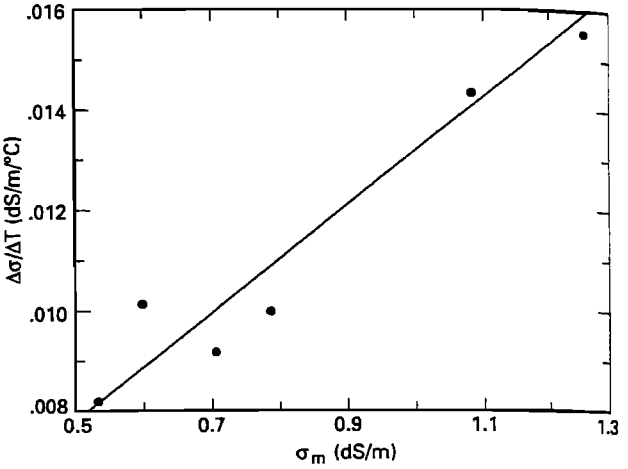

Fig. 4. Temperature sensitivity of electrical conductivity measurements as a function of mean electrical conductivity. Each point was obtained from the slope of the σ versus T relation for a single subsegment after effective hydrostatic equilibrium was achieved. The line is a least squares fit.

viscous enough not to leak out between nonsealed components) of known conductivity (σ_0) filling the cell.

The spatial resolution of electrode configurations can be quantified in terms of a weighting factor w expressing the relative influence of every part of the medium on a σ measurement. The measured U/R in (5) then is considered an integration, over every point r within the sample, of the product of $w(r)$ and $\sigma(r)$. The w factor was determined by measurements of σ with the standard σ solution filling the cell to various heights. Assuming one-dimensional (axial) spatial dependence of this sensitivity and negligible influence from outside the sample, it can be shown that

$$w(x) = \frac{L}{\sigma_0}\frac{d}{dx}\left[\frac{U}{R(x)}\right] \tag{6}$$

where L is the sample height, x is the distance from the center of the electrode set, and $R(x)$ is measured with the top surface of the σ_0 solution at position x. Figure 3 shows point measurements of $w(x)$ with a fit to the Gaussian function

$$w(x) = F \exp(-Gx^2) \tag{7}$$

where F and G have the values 5.4161 and 1.3961 cm^{-2}, respectively.

The measurements show that for the curved square arrangement, 90% of the influence is confined to a region within 9 mm of the center of each square. Measurements with this configuration were treated as point measurements at the center of each square. These three points were 11.3, 19.0, and 26.7 mm from the bottom edge of the retainer.

Temperature Correction

The measured σ is highly dependent on temperature (T), so even the small, periodic variations inside the refrigerated centrifuge (T varying by ±0.2°C around a mean (T_m) of 20.62°C) are significant.

The temperature correction formula used on measured σ values was based on T and σ measurements during a few long data segments at low speed, with the water content effectively stable (at equilibrium). The data for each subsegment showed the uncorrected electrical conductivity (σ_u) to be nearly linear with T. The values of $\Delta\sigma_u/\Delta T$ and $\sigma_m = \sigma_u(T_m)$ computed for these segments are plotted in Figure 4. The essentially linear relation suggested use of the formula

$$\sigma_m = \sigma_u + (D\sigma_u + E)(T_m - T) \tag{8}$$

where D and E are empirically determined parameters. The optimized values of D and E were 0.085°C^{-1} and 0.00355 dS m^{-1} °C^{-1}. Equation (8) was used to convert all of the σ_u data to obtain the temperature-corrected σ_m values which elsewhere in this paper are referred to simply as σ.

Procedure

Each experimental run started with resaturated soil in which entrapped air occupied about 20% of the pore space, as was normal in steady state centrifuge K measurements. The centrifuge was put through a sequence of step increases in speed, with the length of time between steps generally determined by the time needed to approach hydrostatic equilibrium. Theoretical estimates of time to equilibrium, based on numerical solutions of (4), predicted a huge variation, from a few minutes at low speeds to many years at high speeds. Evaporation is a significant complicating factor, hastening the approach to equilibrium water contents while preventing perfectly constant values. In the experiment, various durations of interval between changes were used, ranging from 3 to 72 hours. At speeds less than 100 s^{-1} a reasonable approach to equilibrium was possible.

Table 1 gives the sequence of speeds followed in three separate runs from resaturation. Each step increase determines a data segment, considered here as all the data acquired before the speed changes again. The term "subsegment" designates one set of $\sigma(t)$ or $\theta(t)$, from one of the three measurement positions, over the time of the whole segment. The speed sequences were planned so that most data segments were unique but there was some deliberate replication (e.g., a 46.1–57.6 s^{-1} segment in both runs 1 and 2). Not all

TABLE 1. Sequences of Centrifuge Speeds

Run 1		Run 2		Run 3	
ω, s^{-1}	Acceleration, g	ω, s^{-1}	Acceleration, g	ω, s^{-1}	Acceleration, g
46.1	38.1	14.7	3.9	29.3	15.4
57.6	*59.5*	22.0	8.7	33.5	20.2
70.2	*88.3*	29.3	15.4	36.7	24.1
74.4	99.2	38.7	26.9	38.7	26.9
104.7	196.8	*46.1*	*38.1*	*41.9*	*31.5*
136	333	*57.6*	*59.5*	*46.1*	*38.1*
230	953	*104.7*	*196.8*	*52.4*	*49.2*
				57.6	*59.5*
				70.2	*88.3*

Each run started from $\omega = 0$ with resaturated soil. Italicized numerals are for data segments used for direct comparison with theoretical predictions.

data segments were useful in further analysis, as discussed below.

Electrical measurements were done at various time intervals during each run: once per 25 s just after each speed change, slowing down to as much as 1800 s as the measured quantities change more slowly. Each experimental run produced a $\sigma(t)$ record at three r positions in the sample, as illustrated in Figure 5. Assuming that salinity was reasonably constant and temperature fluctuations were adequately corrected for, the σ results are usable as an indication of θ.

Computation of Water Content

For converting σ to θ, the required calibration function was determined from measurements made at effective hydrostatic equilibrium. The ψ distribution in equilibrium with the centrifugal field is expressed by [*Gardner*, 1937]

$$\psi(r) = (\rho\omega^2/2)(r^2 - r_0^2) \tag{9}$$

where r_0 is the position of the free water surface. With the known $\theta(\psi)$ for Oakley sand (Figure 1*b*), $\theta(r)$ can be readily computed. Then a plot of near-equilibrium σ values (averages typically of 10 to 50 (t, σ) points) versus the computed θ values, as in Figure 6, represents the required data for a $\sigma(\theta)$ calibration. The points in this figure are from all three electrode positions, from centrifuge speeds ranging from 33.5 to 230.4 s^{-1}, with nonequilibrium and experimentally invalid points excluded.

For use as a calibration function, an easily inverted empirical formula

$$\sigma(\theta) = a\theta^b + c \tag{10}$$

where a, b, and c are adjustable parameters, was fitted to the data in Figure 6. This equation is equivalent to equation (5) of *Rhoades et al.* [1976] but with the expression $(a/\sigma_w)\theta^{b-1}$ used for the empirical transmission coefficient. For Oakley sand the best fit values of a, b, and c are 6.4604 dS/m, 2.0343, and 0.023964 dS/m. Goodness of fit, expressed as a multiple correlation coefficient, is 0.9902, and the standard error of estimate is 0.0029 dS/m. Using the inversion of (10), all $\sigma(t)$ data were converted to $\theta(t)$. Figure 7 shows examples of the resulting $\theta(t)$ data segments using point symbols identified in Figure 8.

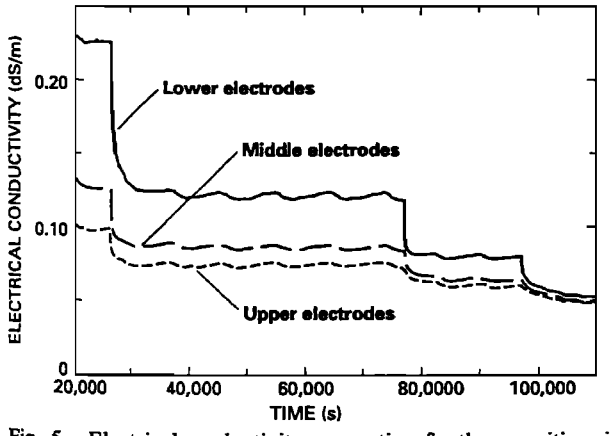

Fig. 5. Electrical conductivity versus time for three positions in the sample during part of run 2, when the speed, starting from 38.7 s^{-1}, was changed to 46.1, 57.6, and 104.7 s^{-1}. The 46.1-s^{-1} segment was prolonged to obtain data used in correcting for evaporation and temperature fluctuations. The σ data here are uncorrected, accounting for the waviness and slight declining bias of the curves.

COMPARISON WITH THEORY

Quality of Data to be Compared

For several reasons, the different $\theta(t)$ subsegments vary in suitability for comparison with theory. Several of the lowest-

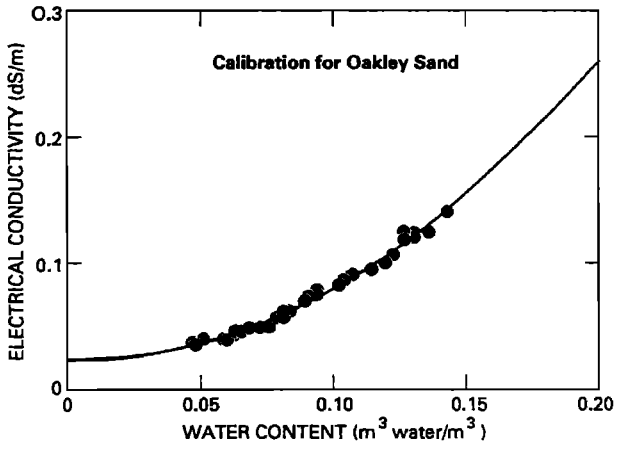

Fig. 6. Electrical conductivity versus water content data with the fitted curve used for calibrating the curved square electrodes.

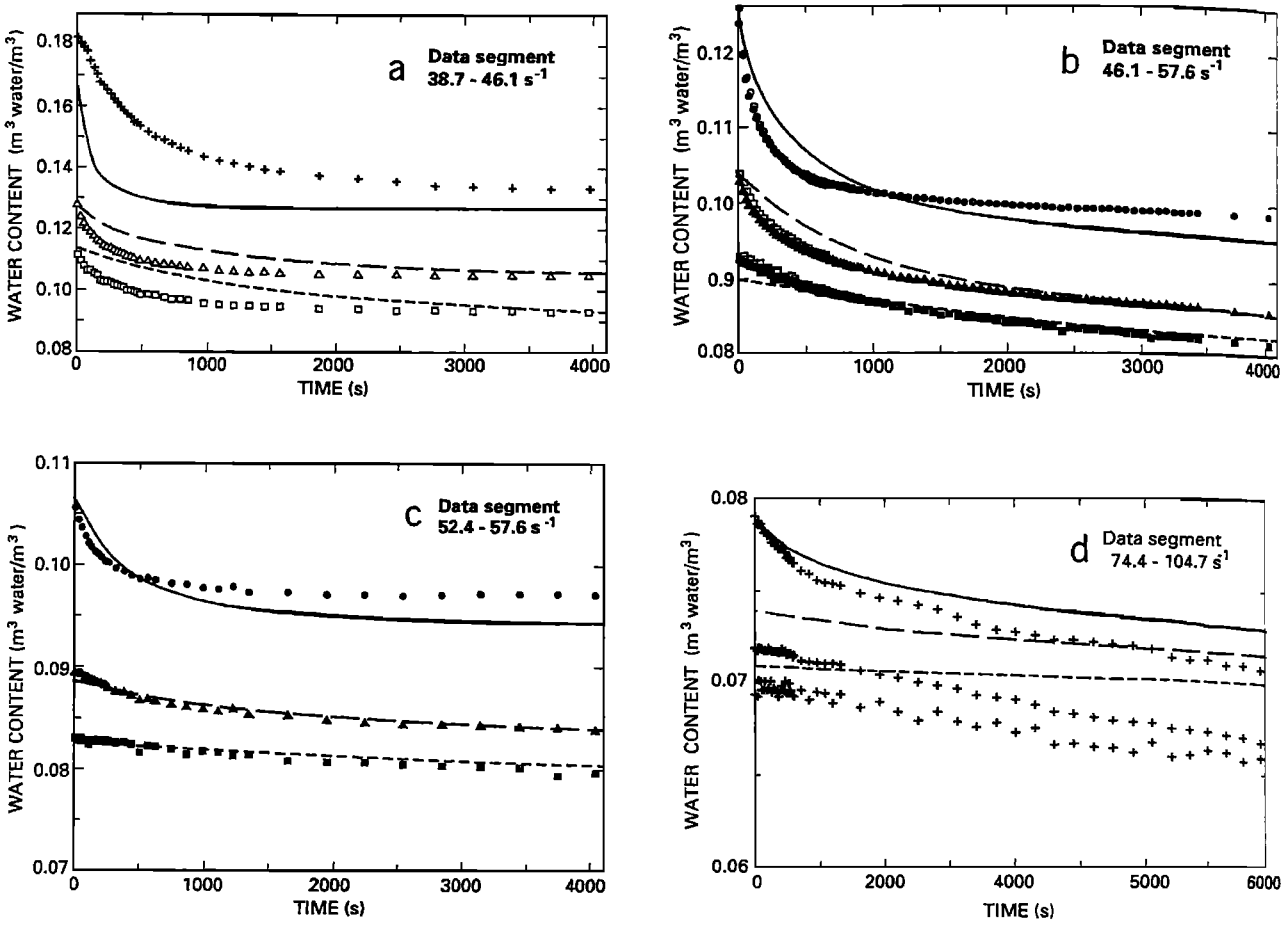

Fig. 7. Selected water content data versus time during equilibration in a centrifugal field. The points, with symbols as explained in the text and in Figure 8, are derived from σ measurements. The curves are computed solutions of Richards' equation. (*a*) The 38.7- to 46.1-s^{-1} segment, showing the low-speed anomaly in which the upper electrode set changes faster than the lower electrode set. (*b*) Two 46.1- to 57.6-s^{-1} segments, superimposed to show the agreement of replication. The segment shown with open symbols (used only to distinguish the two data sets, not to indicate low-speed anomalies) extends only to 700 s. (*c*) The 52.4- to 57.6-s^{-1} segment, in which moisture conditions at all electrode positions were within the range of available accurate K measurements. (*d*) The 74.4- to 104.7-s^{-1} segment, in which moisture conditions were drier than those of available K measurements.

speed segments were discarded immediately because of highly erratic $\theta(t)$ data, which may result from such effects as speed overshoot or poor electrode contact. The highest speeds did not really approach equilibrium in the time available. In Figure 7 it is apparent that other problems are also present, with symptoms related primarily to (1) how close the $\theta(t)$ values are to the range of θ for which K measurements (Figure 1*a*) are available and (2) certain problems that occur at lower speeds. For each of these, called "range effects" and "low-speed effects," respectively, the following criteria are used to assess the quality of the data.

Quality criteria / Electrode set	No speed or range problems	Low speed anomalies	$\bar{\theta}$ out of range
Lower	●	o	+
Middle	▲	△	+
Upper	■	□	+

Fig. 8. Symbols used in Figures 7, 9, and 10 to indicate the three electrode sets and the quality categories of data.

Range effects. To indicate whether excessive extrapolation is required beyond the 0.081–0.117 water content range for which K data are available, the chosen criterion is that $\bar{\theta}$ falls within this range, $\bar{\theta}$ defined as the mean of the initial and final water contents θ_i and θ_f of the subsegment. Those subsegments in Figure 7 which do not meet this criterion are plotted with pluses and are not used in tests of theory.

Low-speed effects, concerning segments with speeds of 52.4 s^{-1} or less. One symptom of problems appears in comparing a given segment with the next higher speed segment. The lower-speed segment, which has wetter soil, should change faster than the higher-speed segment. (The much greater K of the wetter soil easily outweighs the effect of the somewhat weaker driving force.) If instead the lower-speed segment changes more slowly, the anomalous behavior makes it suspect. Segments that show this behavior have data plotted as open symbols. At the lowest speeds the data show an additional symptom: the lowest electrode set,

where the soil is wettest, changes more slowly than the highest electrode set, where the soil is driest (see Figure 7*a*). Possible causes of these low-speed anomalies are discussed later in this paper.

Solution of the Centrifugal Richards' Equation

Equation (4) is a special case of equations solved by *Bear et al.* [1984], the difference being that (4) applies only to an incompressible medium. The present study used the implicit method of Bear et al., starting with the finite difference equation

$$C_j^n\left[\frac{\psi_j^{n+1}-\psi_j^n}{\Delta t}\right]=\frac{1}{(\Delta r)^2}\cdot[K_{j+1}^n\psi_{j+1}^{n+1}-(K_j+K_{j+1}^n)\psi_j^{n+1}+K_j^n\psi_{j-1}^{n+1}]-\frac{1}{\Delta r}(K_{j+1}^n-K_j^n)\rho\omega^2 r_j-K_j^n\rho\omega^2 \quad (11)$$

where C represents specific water capacity $d\theta/d\psi$ of the medium, and n and j are time and space indices, respectively. The required $K(\psi)$ and $\theta(\psi)$ curves (shown in Figure 1) were fitted to data as was done by *Nimmo et al* [1987].

A zero-flux condition was assumed to apply at the top boundary, and two different types of pressure boundary condition were tested for use at the bottom. The simpler of these is based on the assumption that the ceramic plate is infinitely conductive, so that even with finite q the hydrostatic condition of (9) applies within the plate and determines the matric potential ψ_b at the soil-ceramic interface. The alternative boundary condition takes account of the finite plate impedance by adjusting ψ_b by an amount based on a computed excess accumulation of water under conditions where the plate limits the flow. The effective K of the plate was measured to be 3×10^{-7} m/s by the falling-head centrifuge method (J. R. Nimmo and K. A. Mello, Centrifugal measurement of saturated hydraulic conductivity, submitted to *Water Resources Research*, 1990). Using this value in computations, there was little difference between results (a few percent in terms of time dependence) for the two boundary conditions. Results from the limited-flux pressure boundary condition are used in the rest of this paper.

The equation was solved with a grid spacing Δr of 3.81 mm and a time step Δt from 0.1 to 10.0 s, depending on the rate of change of ψ. Initial conditions for each segment were computed from the hydrostatic formula (equation (9)). To simulate actual centrifuge performance, changes in ω were imposed gradually, and with a slight, temporary overshoot, over a period of 20 s. The $\psi(r, t)$ solutions were converted to $\theta(r, t)$ for comparison with measured data. The resulting curves appear in Figure 7.

Quantitative Comparison

A comparison with theory on the basis of the whole curves in Figure 7 would not be strictly valid. The reason is that there are significant calibration-imposed discrepancies between theoretical and experimental endpoints of the curves. The θ_i and θ_f values computed from initial and final σ measurements differ from the theoretical values just as the measured (θ, σ) points in Figure 6 differ from the smooth empirical $\sigma(\theta)$ calibration curve. Thus there is some θ direction shifting and stretching of experimental curves relative to theoretical curves in Figure 7 that reflects imperfections in the calibration rather than in the theory.

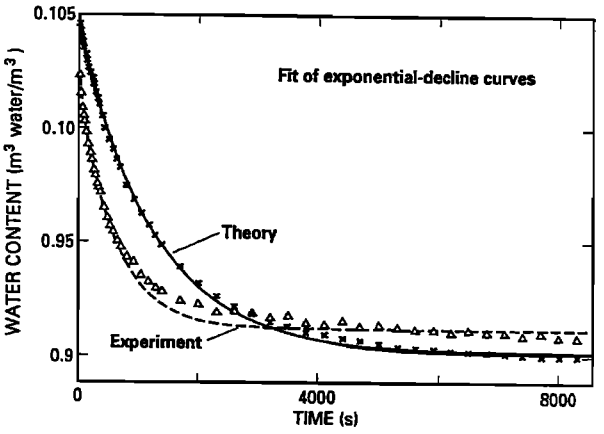

Fig. 9. Exponential decline fits for the middle electrode set in the 46.1- to 52.4-s^{-1} segment. The triangles are experimental data, the crosses are points taken from the theoretical curve and used for fitting, and the curves are fits of the points to formula (12).

The valid comparison of the measured and predicted curves is strictly in their time dependence. For each curve the time dependence was quantified in a way that is insensitive to θ direction deviations in the curves, making use of a simple exponential decline pattern to approximate $\theta(t)$. Physically, using this approximation means that for any given $\theta(t)$, the rate of change is proportional to the amount of water yet to be lost to get to θ_f. Mathematically, it means following the formula

$$\theta(t)=[\theta_i-\theta_f]\exp(-t/\tau)+\theta_f \quad (12)$$

taking $t = 0$ at the time of the step change of speed. The time constant τ is then the desired parameter that quantifies the time dependence. Generally, τ would be expected to vary inversely with K. (The inverse proportionality is exact for solutions of (4) under certain conditions, such as K independent of ψ or $\partial K/\partial r$ proportional to K.) To obtain time constants for comparison, (12) was fitted (optimizing θ_i, θ_f, and τ) to the experimental and theoretical curves using the STARPAC algorithms [*Donaldson and Tryon*, 1983].

For the comparison of τ values to be valid, it is essential to fit the experimental and theoretical cases in an equivalent way. Measured data were first corrected for evaporation. It was assumed that evaporation imposed a constant rate decline on all $\theta(t)$ data. This rate was taken to be 3.23×10^{-8} s^{-1}, determined from the rate of change of θ for a low-speed run long after equilibrium was effectively achieved. Another effect to be considered is that in very long runs the large amount of data in the "tail" region of the curve dominates the curve-fitting process. For this reason all data beyond $t = 15$ hours were excluded. To compute theoretical τ values, exactly as many points were taken for fitting as were available for the experimental fits, and these points were read off of the theoretical curves at the exact t coordinates of the experimental points. Figure 9 shows one example of the exponential decline fitting process.

Of course, the criterion for equivalent time dependence is equality of optimized τ values for experiment and theory.

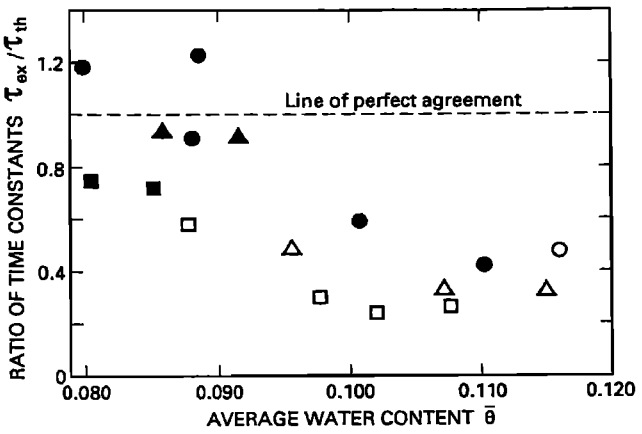

Fig. 10. Comparison of experimental and theoretical time constants. The symbol code is given in Figure 8.

Figure 10 is a graph of the ratio of experimental to theoretical τ, as a function of $\bar{\theta}$. Points of perfect agreement would have a ratio equal to 1.

Discussion

In evaluating the comparison of theory and experiment in Figure 10, the first consideration is that the agreement cannot be expected to be better than the original measured $K(\psi)$ and $\theta(\psi)$ data. Of these, $K(\psi)$ is especially vulnerable to error because it is used in the Richards' equation solution as a fitted empirical formula, necessarily entailing discrepancies from the measurements. The graph of the fitted curve and measured data in Figure 1 shows two additional dashed curves, positioned so that they bracket all the data points. These curves may be represented by multiplying the best fit curve by factors of 1.6 and 0.64. Thus the use of the best fit empirical curve, rather than true data, might easily produce errors of as much as a factor of 1.6. Other sources of quantifiable uncertainty include the 8% measurement error of the K data points, the accuracy of the τ determinations (±15% or better for 95% confidence intervals), errors and fluctuations in centrifuge speed (influencing τ by 5% or less), and errors in the $\theta(\psi)$ measurements that lead to about ±25% errors in $d\theta/d\psi$. The combination of these errors suggests that the agreement should be within a factor of about 2 if Richards' equation, the assumptions concerning conditions within the experiment, and the equivalence of the samples used in the different measurements all are valid.

The results in Figure 10 suggest the following generalizations to be explored further. (1) Agreement between experiment and theory at the lower θ values is as good as could be expected. (2) Most of the experimental measurements indicate a faster changing θ than theory predicts. (3) The degree of agreement appears to be θ dependent, decreasing in wetter soil. (4) The upper electrode set indicates a greater tendency than the other electrodes for experiment to be faster than theory. (5) The data from low-speed segments with anomalous behavior (open symbols) also show experiment to be faster than theory.

The agreement at $\bar{\theta}$ values less than about 0.095, for nearly half of the data, is well within experimental error. On the other hand, the pronounced tendency for τ_{ex} to be less than τ_{th} suggests a systematic physical effect which has not been taken account of. This might indicate a fundamental inadequacy of (4), but it might instead reflect experimental problems which cannot be quantitatively assessed as contributions to measurement uncertainty. Perhaps the most significant effect of this type results from the fact that σ is not really measured at a point, but over a small region of the sample in which θ is not perfectly uniform. During a σ measurement, electrical current flows preferentially through wetter portions within the region of influence, thereby skewing the measurement toward greater θ and faster change. Another possibility is a difference in $K(\psi)$ or $\theta(\psi)$ characteristics between the samples used in the steady state measurements and in the Richards' equation test. Although care was taken to produce equivalent samples, the unsaturated characteristics are so sensitive to treatment that factor of 2 discrepancies, while not expected, are possible. A third problem to consider is unknown variations in the effective impedance of the outflow plate. In particular, the overall effective impedance might be less than was measured if the amount of bypass leakage changes. However, the greater vulnerability to this type of error is not for the observed case but for its inversion, in which a great outflow impedance causes τ_{ex} to exceed τ_{th}.

The θ dependence of the time-constant ratio shows up in that where $\bar{\theta}$ is greater than 0.095, most of the ratios are less than 0.5. The nonquantified systematic effects described above could account for this fact if they are θ-dependent themselves. Effects of imperfect spatial resolution are likely to be greater in wetter soil because of the greater variation in θ within the sample. In the case of characteristic discrepancies between samples, any moisture region could be affected, so to have different K values in wet but not dry soil is certainly possible.

For the top electrodes to indicate a greater discrepancy from theory is not surprising when the overall trend is for experiment to be faster than theory. If the region influencing the top electrode set is considered to have a boundary at, say, the center of the column, and if $\theta(t)$ at that boundary is changing faster during the experiment than is computed in solving (4), this gives an added influence for faster change to the upper, but not the lower, regions of the column.

The anomalous low-speed behavior may result from one or more of the possible but not quantifiable effects discussed above. If there is a problem in knowing the exact effective outflow impedance, it would be more important at low speeds, where the wetter soil has an impedance more nearly equal to that of the outflow plate. Evidence for such an effect appears in the low-speed segment of Figure 7*a*, where the lower electrode set shows an essentially linear decline for about the first 300 s. Additionally, the considerations applying to the upper electrode set are important. They may relate directly to one of the low speed anomalies, namely, the tendency for the three electrode sets to indicate nearly the same rate of change. The upper column effects contribute along with any other mechanisms that may be making these data change faster than predicted. In Figure 10 the upper electrode set accounts for four of the eight open symbol points, including the three lowest values of τ_{ex}/τ_{th}.

Conclusions

Of the 17 points in Figure 10, considering first those that have $\bar{\theta}$ less than 0.095 and show no low-speed anomalies, the

greatest deviation from theory is about 28%, well within experimental error. Considering the whole data set, the greatest deviation from theory is a factor of about 4. While this is twice the factor of 2 discrepancy that quantifiable experimental error could account for, it is not so great that the nonquantifiable effects discussed above could not have caused it. This deviation also is small compared to the degree of error common in measurements at K and θ values as low as those of this study. Thus there is no strong evidence for violations of unsaturated flow theory. The results overall indicate that Richards' equation is valid for the conditions tested. Steady state measurements thus may reasonably predict transient effects, at least when the required accuracy is comparable to that of this test. Because the use of centrifugal force is an extreme case, compared with gravity, and there is no reason to expect this greater force to enhance, rather than degrade, conformance with Richards' equation, this conclusion may be taken to apply to gravity-driven as well as centrifuge-driven flow. It supports the validity of Richards' equation at unusually low K values, of the order of 10^{-10} m/s.

Summarizing important results of this study, it is clear first that the four-electrode curved square configuration permits measurement of electrical conductivity within a small portion of a cylindrical sample. The σ measurements can be calibrated, using a centrifugal field, for conversion to indications of θ. Richards' equation has been confirmed for relatively dry conditions, about one third of saturation, where high-quality steady state K-θ-ψ data are available. Finally, a centrifugal field, at least up to about 200 g, does not invalidate generally accepted unsaturated flow theory.

NOTATION

a, b, c fitted parameters of empirical formula for $\sigma(\theta)$.
C specific water capacity $d\theta/d\psi$.
D, E empirical parameters relating σ and T.
F, G empirical parameters relating w and x.
g acceleration (or force per unit mass) of gravity.
j index of space increments.
K hydraulic conductivity.
L height of sample.
n index of time increments.
r distance from center of rotation.
r_0 value of r at free water surface.
R electrical resistance.
q flux density.
t time.
T temperature.
T_m mean temperature over time.
w weighting function for electrode sensitivity.
x distance from center of electrode configuration.
z vertical space coordinate.
θ water content.
θ_i θ at the beginning of a data segment.
θ_f θ at the end of a data segment.
$\bar{\theta}$ mean of θ_i and θ_f.
ψ matric potential.
Φ_c total potential in a centrifugal field.
Φ_g total potential in a gravitational field.
ρ density of water.
σ electrical conductivity of soil.
σ_0 electrical conductivity of standard solution.
σ_m electrical conductivity at the time-averaged sample temperature.
σ_u electrical conductivity, uncorrected for temperature variations.
τ time constant of exponential decline.
ω angular speed.

Acknowledgments. I am grateful to Catherine Willis for programming the algorithm for solving Richards' equation, and to Katherine Akstin for operating the experimental apparatus for most of the data-taking process.

REFERENCES

Alemi, M. H., D. R. Nielsen, and J. W. Biggar, Determining the hydraulic conductivity of soil cores by centrifugation, *Soil. Sci. Soc. Am. Proc.*, *40*, 212–218, 1976.

Bear, J., M. Y. Corapcioglu, and J. Balakrishna, Modeling of centrifugal filtration in unsaturated deformable porous media, *Adv. Water Resour.*, *7*, 150–167, 1984.

Bresler, E., W. D. Kemper, and R. J. Hanks, Infiltration, redistribution and subsequent evaporation of water from soil as affected by wetting rate and hysteresis, *Soil Sci. Soc. Am. Proc.*, *33*, 832–840, 1969.

Carpenter, E. W., Some notes concerning the Wenner configuration, *Geophys. Prospect.*, *3*, 388–402, 1955.

Donaldson, J. R., and P. V. Tryon, Nonlinear least squares regression using STARPAC, *Tech. Note 1068-2*, 64 pp., Natl. Bur. Stand., Boulder, Colo., 1983.

Freeze, R. A., and J. Banner, The mechanism of natural groundwater recharge and discharge, 2, Laboratory column experiments and field measurements, *Water Resour. Res.*, *6*, 138–155, 1970.

Gardner, R., A method of measuring the capillary tension of soil over a wide moisture range, *Soil Sci.*, *43*, 277, 1937.

Gilham, R. W., A. Klute, and D. F. Heerman, Measurement and numerical simulation of hysteretic flow in a heterogeneous porous medium, *Soil Sci. Soc. Am. J.*, *43*, 1061–1067, 1979.

Gupta, S. C., and R. J. Hanks, Influence of water content on electrical conductivity of the soil, *Soil Sci. Soc. Am. Proc.*, *36*, 855–857, 1972.

Habberjam, G. M., *Apparent Resistivity Observations and the Use of Square Array Techniques*, 149 pp., Geopublication Associates, Berlin, 1979.

Hagoort, J., Oil recovery by gravity drainage, *Soc. Pet. Eng. J.*, *20*, 139–150, 1980.

Hanks, R. J., A. Klute, and E. Bresler, A numeric method for estimating infiltration, redistribution, drainage, and evaporation of water from soil, *Water Resour. Res.*, *5*, 1064–1069, 1969.

Hoa, N. T., R. Gaudu, and C. Thirriot, Influence of the hysteresis effect on transient flows in saturated-unsaturated porous media, *Water Resour. Res.*, *13*, 992–996, 1977.

Kirkham, D., and G. S. Taylor, Some tests of a four-electrode probe for soil moisture measurement, *Soil Sci. Soc. Am. Proc.*, *14*, 42–46, 1950.

Kool, J. B., J. C. Parker, and M. T. van Genuchten, Parameter estimation for unsaturated flow and transport models—A review, *J. Hydrol.*, *91*, 255–293, 1987.

Kunze, R. J., and D. R. Nielsen, Comparison of soil water infiltration profiles obtained experimentally and by solution of Richards' equation, *Soil Sci.*, *135*, 342–349, 1983.

Luthin, J. N., A. Orhun, and G. S. Taylor, Coupled saturated-unsaturated transient flow in porous media: Experimental and numeric model, *Water Resour. Res.*, *11*, 973–978, 1975.

Nimmo, J. R., and K. C. Akstin, Hydraulic conductivity of a sandy soil at low water content after compaction by various methods, *Soil Sci. Soc. Am. J.*, *52*, 303–310, 1988.

Nimmo, J. R., J. Rubin, and D. P. Hammermeister, Unsaturated flow in a centrifugal field: Measurement of hydraulic conductivity and testing of Darcy's law, *Water Resour. Res.*, *23*, 124–134, 1987.

Rhoades, J. D., P. A. C. Raats, and R. J. Prather, Effects of liquid-phase electrical conductivity, water content, and surface conductivity on bulk soil electrical conductivity, *Soil Sci. Soc. Am. J.*, *40*, 651–655, 1976.

Ripple, C. D., R. V. James, and J. Rubin, Radial particle-size segregation during packing of particulates into cylindrical containers, *Powder Technol.*, *8*, 165–175, 1973.

Schofield, A. N., Cambridge geotechnical centrifuge operations, *Geotechnique*, *30*, 227–268, 1980.

Staple, W. J., Comparison of computed and measured moisture redistribution following infiltration, *Soil Sci. Soc. Am. Proc.*, *33*, 840–847, 1969.

Tang, Y. K., and R. W. Skaggs, Experimental evaluation of theoretical solutions for subsurface drainage and irrigation, *Water Resour. Res.*, *13*, 957–965, 1977.

Topp, G. C., Surface tension and water contamination as related to the selection of flow system components, *Soil Sci. Soc. Am. Proc.*, *30*, 128–129, 1966.

van Spronsen, E., Three-phase relative permeability measurements using the centrifuge method, Proceedings of the Third Joint SPE/DOE Symposium on Enhanced Oil Recovery, *Rep. SPE/DOE 10688*, pp. 217–240, Soc. of Pet. Eng./Dep. of Energy, Tulsa, Okla., 1982.

J. R. Nimmo, Water Resources Division, U.S. Geological Survey, 345 Middlefield Road, Mail Stop 421, Menlo Park, CA 94025.

(Received November 16, 1989;
revised April 20, 1990;
accepted April 26, 1990.)